

1N-32-CR

115497

P.21



## HIGH-FREQUENCY TECHNIQUES FOR RCS PREDICTION OF PLATE GEOMETRIES

Semiannual Progress Report

Constantine A. Balanis and Lesley A. Polka

February 1, 1992 - July 31, 1992

(NASA-CR-190656) HIGH-FREQUENCY  
TECHNIQUES FOR RCS PREDICTION OF  
PLATE GEOMETRIES Semiannual  
Progress Report, 1 Feb. - 31 Jul.  
1992 (Arizona State Univ.) 21 p

N92-31273

Unclass

G3/32 0115497

**Telecommunications Research Center  
College of Engineering and Applied Science  
Arizona State University  
Tempe, AZ 85287-7206**

Grant No. NAG-1-562  
National Aeronautics and Space Administration  
Langley Research Center  
Hampton, VA 23665



# **HIGH-FREQUENCY TECHNIQUES FOR RCS PREDICTION OF PLATE GEOMETRIES**

Semiannual Progress Report

Constantine A. Balanis and Lesley A. Polka

February 1, 1992 - July 31, 1992

Telecommunications Research Center  
College of Engineering and Applied Science  
Arizona State University  
Tempe, AZ 85287-7206

Grant No. NAG-1-562  
National Aeronautics and Space Administration  
Langley Research Center  
Hampton, VA 23665

## Abstract

This report presents hard polarization diffraction coefficients for the special case of a wedge that is coated with a lossy dielectric on one face and is perfectly conducting on the other face. Expressions for plane-wave incidence, far-field observation; for cylindrical-wave incidence, far-field observation; and for plane-wave incidence, near-field observation are presented for regular diffractions. In addition, terms for surface-wave and surface-wave transition fields are presented. These expressions are derived from the UTD coefficients for a generalized impedance wedge and are simplified for rapid calculation for the case of one perfectly conducting face. Results from a first-order model for a coated, rectangular plate are examined; and potential problems in extending this modeling approach to more complicated coated structures are identified.

# I. INTRODUCTION

One of the most relevant topics in the area of high-frequency asymptotic techniques for scattering prediction is the development of accurate theories for perfectly conducting geometries covered with thin, lossy coatings. Techniques such as GTD/UTD [1], [2] and PTD [3], [4] have reached a high level of sophistication and maturity in the realm of perfectly conducting geometries. Furthermore, work on the UTD for the dielectric wedge has advanced to the point that general, computationally tractable coefficients are available for all wedge angles [5] - [7] and have been applied to practical geometries [8]. Developing UTD expressions for coated geometries is an important follow-up topic as coated geometries have more practical applications than the more ideal perfectly conducting and dielectric wedge geometries. Practical applications of the coated geometry are in low-observable vehicles, collision-avoidance systems, and communications satellites.

The most difficult inherent problem in accurately modeling coated structures is developing accurate, easily implemented, computationally fast expressions for the coating impedance. Previous reports [9] - [13] have explored methods for applying the UTD impedance wedge coefficients to a coated wedge and a coated plate. The coefficients have successfully been adapted and simplified for the special case of plane-wave incidence, far-field observation, hard polarization; and these coefficients have been used to develop a first-order, hard polarization model for the coated plate that agrees quite well with experimental results considering the primitiveness of the model [13].

This report continues in this area by presenting UTD expressions for the hard polarization case for regular diffractions for plane-wave incidence, far-field observation; cylindrical-wave incidence from a source at a finite distance, far-field observation; and plane-wave incidence, near-field observation. Furthermore, expressions

for surface waves and surface-wave transition fields are also given. Results from a first-order model using these diffraction coefficients for a coated, rectangular plate are presented and discussed.

## II. THEORY AND RESULTS

### A. Problem Geometries and Parameters

The two geometries analyzed in this report are shown in Figs. 1 and 2. The impedance wedge shown in Fig. 1 is the two-dimensional canonical, infinite wedge for which the impedance UTD diffraction coefficients are derived. Fig. 1 demonstrates the plane-wave incidence, far-field observation case with incidence angle,  $\psi'$ , and observation angle,  $\psi$ . Cylindrical-wave incidence from a source at a finite distance,  $\rho'$ , from the edge of the wedge will also be considered when the observation point is in the far field. The reciprocal case of plane-wave incidence, observation at a finite distance,  $\rho$ , from the wedge edge will also be included. The interior angle of the wedge is designated as  $(2 - n)\pi$  so that, for example, a half plane is designated by a wedge parameter of  $n = 2$ . The top face is face “0” and the bottom is face “ $n$ ”.

The research in this report is primarily concerned with thin coatings on perfectly conducting surfaces so that the wedge geometry analyzed in the report has a perfectly conducting “ $n$ ” face. The parameter used to describe the wedge faces is the surface impedance,  $\eta$ . For the perfectly conducting “ $n$ ” face the surface impedance is zero. The impedance of the “0” face is not so simply represented. Future work will explore higher-order boundary conditions and other methods for modeling a coating on a perfectly conducting surface; however, this report uses a shorted-transmission-line approximation for the coating impedance. This is accurate near and at normal incidence to the surface and is a relatively simple model

to incorporate into the UTD diffraction coefficients. The equivalent impedance of the coated “0” face normalized with respect to the impedance of free-space is represented as:

$$\eta_0 = j \sqrt{\frac{\mu_{r0}}{\epsilon_{r0}}} \tan(2\pi \sqrt{\mu_{r0} \epsilon_{r0}} t) \quad (1)$$

where  $\mu_{r0}$  and  $\epsilon_{r0}$  are the relative permeability and the relative permittivity, respectively, of the “0” face; and  $t$  is the coating thickness in free-space wavelengths.

The equivalent surface impedance for each of the wedge faces is used to determine the Brewster angle,  $\theta$ , for that surface, where the Brewster angle is the angle at which no reflection is present. The Brewster angle is polarization dependent and is given by:

#### Hard Polarization

$$\theta = \sin^{-1}(\eta) \quad (2)$$

#### Soft Polarization

$$\theta = \sin^{-1}\left(\frac{1}{\eta}\right) \quad (3)$$

$\eta$  is the impedance of the surface normalized with respect to the free-space impedance. Since the coatings in this study are lossy and thus have complex permeabilities, the Brewster angles are also complex.

The coated, rectangular plate model is shown in Fig. 2. The width of the plate is  $w$ , and the length is  $L$ ; the coating thickness is  $t$ . The incidence angle with respect to the x-y axis is  $\phi'$ , and the observation angle is  $\phi$ . The incidence and observation angles with respect to the left edge of the plate are  $\psi'_1$  and  $\psi_1$ , respectively. With respect to the right edge, the incidence and observation angles

are  $\psi'_2$  and  $\psi_2$ , respectively.

## B. Coefficients for Hard Polarization

### 1. Plane-Wave Incidence, Far-Field Observation

The general UTD diffraction coefficient is given in [14] as:

$$\begin{aligned}
D(\rho, \phi', \phi, \theta_0, \theta_n, n) = & \frac{-e^{-j\frac{\pi}{4}}}{2n\sqrt{2\pi k}} \left\{ \frac{\psi(-\pi + \frac{n\pi}{2} - \phi)}{\psi(\frac{n\pi}{2} - \phi')} \frac{\sin(\frac{\phi'}{n}) + \sin(\frac{\theta_0}{n})}{\sin(\frac{\phi+\pi}{n}) + \sin(\frac{\theta_0}{n})} \right. \\
& \times \cot\left(\frac{\pi + \beta^-}{2n}\right) F\left[k\rho\left(1 + \cos\left(\beta^- - 2n\pi N_-^+\right)\right)\right] \\
& + \frac{\psi(\pi + \frac{n\pi}{2} - \phi)}{\psi(\frac{n\pi}{2} - \phi')} \frac{\sin(\frac{\phi'}{n}) + \sin(\frac{\theta_0}{n})}{\sin(\frac{\phi-\pi}{n}) + \sin(\frac{\theta_0}{n})} \\
& \times \cot\left(\frac{\pi - \beta^-}{2n}\right) F\left[k\rho\left(1 + \cos\left(\beta^- - 2n\pi N_-^-\right)\right)\right] \\
& + \frac{\psi(-\pi + \frac{n\pi}{2} - \phi)}{\psi(\frac{n\pi}{2} - \phi')} \frac{\sin(\frac{\phi'}{n}) - \sin(\frac{\theta_0}{n})}{\sin(\frac{\phi+\pi}{n}) + \sin(\frac{\theta_0}{n})} \\
& \times \cot\left(\frac{\pi + \beta^+}{2n}\right) F\left[k\rho\left(1 + \cos\left(\beta^+ - 2n\pi N_+^+\right)\right)\right] \\
& + \frac{\psi(\pi + \frac{n\pi}{2} - \phi)}{\psi(\frac{n\pi}{2} - \phi')} \frac{\sin(\frac{\phi'}{n}) - \sin(\frac{\theta_0}{n})}{\sin(\frac{\phi-\pi}{n}) + \sin(\frac{\theta_0}{n})} \\
& \times \cot\left(\frac{\pi - \beta^+}{2n}\right) F\left[k\rho\left(1 + \cos\left(\beta^+ - 2n\pi N_+^-\right)\right)\right] \left. \right\} \quad (4)
\end{aligned}$$

where

$$\beta^\pm = \phi \pm \phi' \quad (5)$$

$F(x)$  is the Fresnel transition function defined in [2] as:

$$F(x) = 2j\sqrt{x}e^{jx} \int_{\sqrt{x}}^{\infty} e^{-j\tau^2} d\tau \quad (6)$$

and the  $N$ 's are integers that most closely satisfy:

$$2\pi n N_-^+ - \beta^- = \pi \quad (7)$$

$$2\pi n N_-^- - \beta^- = -\pi \quad (8)$$

$$2\pi n N_+^+ - \beta^+ = \pi \quad (9)$$

$$2\pi n N_+^- - \beta^+ = -\pi \quad (10)$$

This coefficient is valid for plane-wave incidence, observation at a finite distance,  $\rho$ , from the edge of the wedge.

$\psi(z)$  is the auxiliary Maliuzhinets function, defined as:

$$\begin{aligned} \psi(z) = & \psi_n(z + \frac{n\pi}{2} + \frac{\pi}{2} - \theta_0) \psi_n(z - \frac{n\pi}{2} - \frac{\pi}{2} + \theta_n) \\ & \times \psi_n(z + \frac{n\pi}{2} - \frac{\pi}{2} + \theta_0) \psi_n(z - \frac{n\pi}{2} + \frac{\pi}{2} - \theta_n) \end{aligned} \quad (11)$$

or, alternatively, as:

$$\begin{aligned} \psi(z) = & \left[ \psi_n\left(\frac{\pi}{2}\right) \right]^4 \cos\left(\frac{z + \frac{n\pi}{2} - \theta_0}{2n}\right) \cos\left(\frac{z - \frac{n\pi}{2} + \theta_n}{2n}\right) \\ & \times \frac{\psi_n(z + \frac{n\pi}{2} - \frac{\pi}{2} + \theta_0) \psi_n(z - \frac{n\pi}{2} + \frac{\pi}{2} - \theta_n)}{\psi_n(z + \frac{n\pi}{2} - \frac{\pi}{2} - \theta_0) \psi_n(z - \frac{n\pi}{2} + \frac{\pi}{2} + \theta_n)} \end{aligned} \quad (12)$$



$\psi_n(z)$  is the Maliuzhinets function given by:

$$\psi_n(z) = \exp \left[ -\frac{1}{2} \int_0^\infty \frac{\cosh(zs) - 1}{s \cosh(\frac{\pi}{2}s) \sinh(n\pi s)} ds \right] \quad (13)$$

This integral is approximated in this work using a 200-point Riemann sum over the interval from 0 to 8 and the recursion relations of [15]; *i.e.*, the integral is approximated as:

$$\psi_n(z) \cong \exp \left[ -\frac{1}{2} \int_0^8 \frac{\cosh(zs) - 1}{s \cosh(\frac{\pi}{2}s) \sinh(n\pi s)} ds \right] \quad (14)$$

The general diffraction coefficient of (4) can be greatly simplified for coated geometries for which the impedance of the “ $n$ ” face is zero. Simplifying the diffraction coefficient leads to faster computation times and will make it easier to incorporate more accurate expressions for the coating impedance in future work. For plane-wave incidence, far-field observation the Fresnel transition functions in (4) are approximated as 1. As was demonstrated in the previous report [13], for the hard polarization, coated case, the diffraction coefficient simplifies to:

$$\begin{aligned} D(\phi', \phi, \theta_0^h, n) = & \left[ \frac{-e^{-j\frac{\pi}{4}}}{2n\sqrt{2\pi k}} \right] \left\{ \frac{1}{\cos\left(\frac{\phi'}{2n}\right) \sin\left(\frac{\phi' + \theta_0^h}{2n}\right)} \right\} \frac{\psi_n\left(-\frac{\pi}{2} + n\pi - \phi' - \theta_0^h\right)}{\psi_n\left(-\frac{\pi}{2} + n\pi - \phi' + \theta_0^h\right)} \\ & \times \left\{ \frac{\psi_n\left(-\frac{3\pi}{2} + n\pi - \phi + \theta_0^h\right) \cos\left(\frac{\pi + \phi}{2n}\right)}{\psi_n\left(-\frac{3\pi}{2} + n\pi - \phi - \theta_0^h\right) \cos\left(\frac{\pi + \phi - \theta_0^h}{2n}\right)} \right\} \end{aligned}$$

$$\begin{aligned}
& \times \left[ \cos \left( \frac{\phi' - \theta_0^h}{2n} \right) \sin \left( \frac{\phi' + \theta_0^h}{2n} \right) \cot \left( \frac{\pi + \beta^-}{2n} \right) \right. \\
& + \sin \left( \frac{\phi' - \theta_0^h}{2n} \right) \cos \left( \frac{\phi' + \theta_0^h}{2n} \right) \cot \left( \frac{\pi + \beta^+}{2n} \right) \left. \right] \\
& + \frac{\psi_n \left( \frac{\pi}{2} + n\pi - \phi + \theta_0^h \right) \cos \left( \frac{\pi - \phi}{2n} \right)}{\psi_n \left( \frac{\pi}{2} + n\pi - \phi - \theta_0^h \right) \cos \left( \frac{\pi - \phi + \theta_0^h}{2n} \right)} \\
& \times \left[ \cos \left( \frac{\phi' - \theta_0^h}{2n} \right) \sin \left( \frac{\phi' + \theta_0^h}{2n} \right) \cot \left( \frac{\pi - \beta^-}{2n} \right) \right. \\
& + \sin \left( \frac{\phi' - \theta_0^h}{2n} \right) \cos \left( \frac{\phi' + \theta_0^h}{2n} \right) \cot \left( \frac{\pi - \beta^+}{2n} \right) \left. \right] \Bigg\} \quad (15)
\end{aligned}$$

This simplified version of the impedance-wedge diffraction coefficient is analogous to the Keller GTD diffraction coefficient [1] for the perfectly conducting wedge.

## 2. Plane-Wave Incidence, Observation at a Finite Distance

In order to incorporate higher-order diffraction terms into target models, *e. g.*, the coated strip of Fig. 2, a simplified version of (4) is needed in which the Brewster angle for the “ $n$ ” face is set to 0. Substituting  $\theta_n = 0$  and using the identity from (12), the resulting diffraction coefficient is:

$$\begin{aligned}
D(\phi', \phi, \theta_0^h, n) &= \left[ \frac{-e^{-j\frac{\pi}{4}}}{2n\sqrt{2\pi k}} \right] \left\{ \frac{1}{\cos \left( \frac{\phi'}{2n} \right) \sin \left( \frac{\phi' + \theta_0^h}{2n} \right)} \right\} \frac{\psi_n \left( -\frac{\pi}{2} + n\pi - \phi' - \theta_0^h \right)}{\psi_n \left( -\frac{\pi}{2} + n\pi - \phi' + \theta_0^h \right)} \\
&\times \left\{ \frac{\psi_n \left( -\frac{3\pi}{2} + n\pi - \phi + \theta_0^h \right) \cos \left( \frac{\pi + \phi}{2n} \right)}{\psi_n \left( -\frac{3\pi}{2} + n\pi - \phi - \theta_0^h \right) \cos \left( \frac{\pi + \phi - \theta_0^h}{2n} \right)} \right. \\
&\times \left[ \cos \left( \frac{\phi' - \theta_0^h}{2n} \right) \sin \left( \frac{\phi' + \theta_0^h}{2n} \right) \cot \left( \frac{\pi + \beta^-}{2n} \right) \right.
\end{aligned}$$

$$\begin{aligned}
& \times F \left[ k\rho \left( 1 + \cos(\beta^- - 2n\pi N_-^+) \right) \right] \\
& + \sin \left( \frac{\phi' - \theta_0^h}{2n} \right) \cos \left( \frac{\phi' + \theta_0^h}{2n} \right) \cot \left( \frac{\pi + \beta^+}{2n} \right) \\
& \times F \left[ k\rho \left( 1 + \cos(\beta^+ - 2n\pi N_+^+) \right) \right] \\
& + \frac{\psi_n \left( \frac{\pi}{2} + n\pi - \phi + \theta_0^h \right) \cos \left( \frac{\pi - \phi}{2n} \right)}{\psi_n \left( \frac{\pi}{2} + n\pi - \phi - \theta_0^h \right) \cos \left( \frac{\pi - \phi + \theta_0^h}{2n} \right)} \\
& \times \left[ \cos \left( \frac{\phi' - \theta_0^h}{2n} \right) \sin \left( \frac{\phi' + \theta_0^h}{2n} \right) \cot \left( \frac{\pi - \beta^-}{2n} \right) \right. \\
& \times F \left[ k\rho \left( 1 + \cos(\beta^- - 2n\pi N_-^-) \right) \right] \\
& + \sin \left( \frac{\phi' - \theta_0^h}{2n} \right) \cos \left( \frac{\phi' + \theta_0^h}{2n} \right) \cot \left( \frac{\pi - \beta^+}{2n} \right) \\
& \left. \times F \left[ k\rho \left( 1 + \cos(\beta^+ - 2n\pi N_+^-) \right) \right] \right] \} \tag{16}
\end{aligned}$$

As for the coefficient in (15), the number of Maliuzhinets functions which must be calculated has been reduced from 12 in (4) to 6. This greatly speeds up computation time because each Maliuzhinets function requires numerical integration.

### 3. Cylindrical-Wave Incidence, Far-Field Observation

A diffraction coefficient for cylindrical-wave incidence from a source at a distance  $\rho'$  from the edge of the wedge, observation in the far field is also necessary in determining higher-order diffraction mechanisms from objects with two parallel edges. This coefficient can be obtained from the expression in the previous section by reciprocity; *i. e.* , by substituting  $\rho'$  for  $\rho$  and switching  $\phi$  and  $\phi'$  in (16).

#### 4. Surface-Wave Terms

Surface-wave fields originate at the point of diffraction on an impedance wedge and propagate along the surface of the wedge. Although they decay rapidly along the wedge face, they can be a major contribution to higher-order diffracting fields and should be considered in any model of a complicated geometry. Surface waves exist only over a limited angular region given by:

$$-\pi < \left[ \alpha_{r_0} - \cos^{-1} \left( \frac{1}{\cosh(\alpha_{i_0})} \right) \operatorname{sgn}(\alpha_{i_0}) \right] < \pi \quad (17)$$

where

$$\alpha_0 = \alpha_{r_0} + j\alpha_{i_0} = \phi + \pi + \theta_0 \quad (18)$$

The above expressions are for the “0” face of the wedge. For the coated wedge considered in this work, the “n” face is perfectly conducting and cannot, therefore, support surface waves.

The expression for the surface wave that exists on the “0” face of a general impedance wedge is [14]:

$$\begin{aligned} U_{sw}^0 &= U_0 \frac{2 \sin \left( \frac{\pi}{2n} \right)}{\psi \left( \frac{n\pi}{2} - \phi' \right)} \left[ \frac{\sin \left( \frac{\phi'}{n} \right)}{\cos \left( \frac{\pi + \theta_0}{n} \right) - \cos \left( \frac{\phi'}{n} \right)} \right] e^{-jk\rho \cos(\phi + \theta_0)} \\ &\quad \psi_n \left( n\pi - \frac{\pi}{2} \right) \psi_n \left( \frac{\pi}{2} + n\pi + 2\theta_0 \right) \\ &\quad \times \psi_n \left( \frac{3\pi}{2} + \theta_0 - \theta_n \right) \psi_n \left( \frac{\pi}{2} + \theta_0 + \theta_n \right) \end{aligned} \quad (19)$$

For the hard polarization case for the coated wedge this expression simplifies to:

$$\begin{aligned}
U_{sw}^0 = & -2U_0 \frac{\sin\left(\frac{\pi}{2n}\right) \sin\left(\frac{\phi'}{2n}\right) \cos\left(\frac{\pi+\theta_0}{2n}\right) e^{-jk\rho \cos(\phi+\theta_0)}}{\cos\left(\frac{n\pi-\phi'-\theta_0}{2n}\right) \sin\left(\frac{\pi+\theta_0+\phi'}{2n}\right) \sin\left(\frac{\pi+\theta_0-\phi'}{2n}\right)} \\
& \times \frac{\psi_n(n\pi - \frac{\pi}{2}) \psi_n(\frac{\pi}{2} + n\pi + 2\theta_0) \psi_n(n\pi - \phi' - \frac{\pi}{2} - \theta_0)}{\left[\psi_n(\frac{\pi}{2})\right]^2 \psi_n(n\pi - \phi' - \frac{\pi}{2} + \theta_0)} \quad (20)
\end{aligned}$$

The above expression assumes plane-wave incidence and observation at a finite distance,  $\rho$ . This term should be used to calculate only second-order diffractions due to surface waves. A mathematically sound method for determining higher-order diffractions due to surface waves using the UTD for impedance wedges has not yet been found.

Since the surface wave terms exist over a finite angular range, a surface wave transition boundary, at which a discontinuity occurs, exists. This is similar to the incident and reflected ray boundaries in Geometrical Optics (GO). Just as the UTD field corrects for GO discontinuities, the surface-wave transition field corrects for discontinuities in the surface-wave field. The surface-wave transition field for the “0” face of a general impedance wedge is [7]:

$$\begin{aligned}
U_{swtr}^0 = & U_0 \frac{e^{-jk\rho}}{\sqrt{\rho}} \left[ \frac{-\sqrt{\frac{2}{\pi}} \sin(\frac{\pi}{2n})}{\psi(\frac{n\pi}{2} - \phi')} \right] \frac{\sin(\frac{\phi'}{n})}{\cos(\frac{\pi+\theta_0}{n}) - \cos(\frac{\phi'}{n})} \\
& \frac{[F[k\rho(1 - \cos(\phi + \theta_0))] - 1]}{\sqrt{k(\cos(\phi + \theta_0) - 1)}} \\
& \psi_n(n\pi - \frac{\pi}{2}) \psi_n(\frac{\pi}{2} + n\pi + 2\theta_0) \\
& \times \psi_n(\frac{3\pi}{2} + \theta_0 - \theta_n) \psi_n(\frac{\pi}{2} + \theta_0 + \theta_n) \quad (21)
\end{aligned}$$

For the coated wedge, hard polarization case, this simplifies to:

$$\begin{aligned}
U_{swtr}^0 = U_0 \frac{e^{-jk\rho}}{\sqrt{k\rho}} & \left\{ \frac{\sqrt{\frac{j}{\pi}} \sin(\frac{\pi}{2n}) \sin(\frac{\phi'}{2n}) \cos(\frac{\pi+\theta_0}{2n})}{\sqrt{\cos(\phi+\theta_0)-1} \cos(\frac{n\pi-\phi'-\theta_0}{2n})} \right. \\
& \times \frac{[F[k\rho(1-\cos(\phi+\theta_0))]-1]}{\sin(\frac{\pi+\theta_0+\phi'}{2n}) \sin(\frac{\pi+\theta_0-\phi'}{2n})} \left. \right\} \\
& \times \frac{\psi_n(n\pi - \frac{\pi}{2}) \psi_n(\frac{\pi}{2} + n\pi + 2\theta_0) \psi_n(n\pi - \phi' - \frac{\pi}{2} - \theta_0)}{\left[\psi_n(\frac{\pi}{2})\right]^2 \psi_n(n\pi - \phi' - \frac{\pi}{2} + \theta_0)} \quad (22)
\end{aligned}$$

The Fresnel transition function in the above expression has a complex argument; therefore, in calculations, this is the same function as in (6) except that it has been extended to the complex plane. This function and methods for its calculation are described in [14].

## 5. Results

The diffraction coefficients that were presented above will be incorporated into a model for the coated plate geometry of Fig. 2 in future work. This model will include higher-order diffraction terms and surface-wave terms. At this point, a first-order model has been implemented. Results from this model for the hard polarization are compared to measured data in Fig. 3. The plate dimensions are  $2\lambda \times 2\lambda$  at 10 GHz. The coating thickness is  $t = 0.0423\lambda$ , and the material parameters of the coating are  $\mu_{r0} = 1.539 - j1.2241$  and  $\epsilon_{r0} = 11.826 - j0.16639$ . The theoretical results are in good agreement with the experimental results considering the primitiveness of the model. Discontinuities and discrepancies near and at the grazing angles ( $\phi = 0^\circ, 180^\circ$ , and  $360^\circ$ ) will undoubtedly be mitigated with the addition of higher-order terms and surface-wave terms.

The area of disagreement between the theoretical data and the measured data that is of greatest concern is the area around  $\phi = 45^\circ$  and  $\phi = 135^\circ$  on the coated

side of the plate. The disagreement in these areas is large, and it is not evident that the addition of higher-order terms will resolve the differences. This is a critical scattering angle in the modeling of the coated  $90^\circ$  dihedral corner reflector because this angle corresponds to the angle of incidence with respect to the two plates comprising the reflector when the backscattered field from the reflector is greatest. Accurate modeling of the coated dihedral corner reflector depends, therefore, on accurate modeling of the coated plate at  $\phi = 45^\circ$  and  $\phi = 135^\circ$ . The equation (1) for the coating impedance may not be a sufficient model at this angle because this formulation is intended for use near and at normal incidence to the plate. Higher-order boundary conditions may be necessary in modeling the coating for angles away from normal incidence. This will be investigated in future work.

### III. FUTURE WORK

Immediate future work will entail formulating a more sophisticated coated plate model that includes higher-order diffractions and surface-wave terms. Terms up to fourth order will be added. Work on the perfectly conducting, rectangular plate has shown that terms of order higher than fourth order are very insignificant contributors to the total scattered field [12].

The coated wedge coefficients and coated plate model will also be extended to the soft polarization case. For this case the Brewster angle for the “ $n$ ” face, given in (3), is infinite. Formulating the coefficients for this case is not as straightforward as for the hard polarization case. This problem is currently under investigation.

Although adding higher-order terms will probably improve the coated plate to a certain degree, a higher-order boundary condition is obviously needed for modeling the coating boundary conditions at angles away from normal incidence, as was indicated by the results in Fig. 3. Several different approaches to developing generalized impedance boundary conditions (GIBC's) have been presented in the

recent literature [16] - [18]. These methods will be explored and applied to the coated plate geometry.

Just as for the perfectly conducting plate geometry, overlapping transition regions that appear at and near grazing incidence are problem areas in which the UTD cannot be applied in its traditional form. This problem and its solution are explored by Tiberio, *et al.* [19]. This solution will be incorporated into the general, coated plate solution in the future.

Eventually, the work on coated geometries will be extended to more complicated, general problems, specifically the coated dihedral corner reflector and the rotated coated plate (*i.e.*, scattering in off-principal planes). In the off-principal plane case it will be necessary to explore hybrid methods such as the MM/PO approach presented by Bilow [20]. This and other appropriate solutions will be investigated in future work.



## References

- [1] J. B. Keller, "Geometrical theory of diffraction," *J. Opt. Soc. Amer.* , vol. 52, pp. 116-130, Feb. 1962.
- [2] R. G. Kouyoumjian and P. H. Pathak, "A uniform geometrical theory of diffraction for an edge in a perfectly conducting surface," *Proc. IEEE*, vol. 62, pp. 1448-1461, Nov. 1974.
- [3] P. I. Ufimtsev, "Approximate computation of the diffraction of plane electromagnetic waves at certain metal bodies: I. Diffraction patterns at a wedge and a ribbon," *Sov. Phys. - Tech. Phys.* , vol. 27, pp. 1708-1718, 1957.
- [4] —, "Secondary diffraction of electromagnetic waves by a strip," *Sov. Phys. - Tech. Phys.* , vol. 28. , pp. 535-548, 1958.
- [5] G. D. Maluizhinets, "Excitation, reflection, and emission of surface waves from a wedge with given face impedances," *Sov. Phys. Doklady*, vol. 3, pp. 752-755, Jul. /Aug. 1958.
- [6] R. Tiberio, G. Pelosi, and G. Manara, "A uniform GTD formulation for the diffraction by a wedge with impedance faces," *IEEE Trans. Antennas Propagat.* , vol. AP-33, pp. 867-873, Aug. 1985.
- [7] T. Griesser and C. A. Balanis, "Reflections, diffractions, and surface waves for an impedance wedge of arbitrary angle," *IEEE Trans. Antennas Propagat.* , vol. AP-37, pp. 927-935, Jul. 1989.
- [8] T. Griesser, C. A. Balanis, and K. Liu, "RCS analysis and reduction for lossy dihedral corner reflectors," *Proc. IEEE*, vol. 77, pp. 806-814, May 1989.
- [9] C. A. Balanis, L. A. Polka, and K. Liu, "Nonprincipal-plane scattering from rectangular plates and pattern control of horn antennas," Semiannual Report, Grant No. NAG-1-562, National Aeronautics and Space Administration, Langley Research Center, Hampton, VA, Jan. 31, 1990.
- [10] —, "Scattering from coated structures and antenna pattern control using impedance surfaces," Semiannual Report, Grant No. NAG-1-562, National Aeronautics and Space Administration, Langley Research Center, Hampton, VA, Jul. 31, 1990.

- [11] C. A. Balanis and L. A. Polka, "High-frequency techniques for RCS prediction of plate geometries," Semiannual Report, Grant No. NAG-1-562, National Aeronautics and Space Administration, Langley Research Center, Hampton, VA, Jan. 31, 1991.
- [12] —, "High-frequency techniques for RCS prediction of plate geometries," Semiannual Report, Grant No. NAG-1-562, National Aeronautics and Space Administration, Langley Research Center, Hampton, VA, Jul. 31, 1991.
- [13] —, "High-frequency techniques for RCS prediction of plate geometries," Semiannual Report, Grant No. NAG-1-562, National Aeronautics and Space Administration, Langley Research Center, Hampton, VA, Jan. 31, 1992.
- [14] T. Griesser, "High-frequency electromagnetic scattering from imperfectly conducting structures," Ph. D. dissertation, Arizona State University, Tempe, Arizona, Aug. 1988.
- [15] M. I. Herman, J. L. Volakis, and T. B. A. Senior, "Analytic expressions for a function occurring in diffraction theory," *IEEE Trans. Antennas Propagat.*, vol. AP-35, 1083-1086, Sept. 1987.
- [16] R. G. Rojas, "Generalised impedance boundary conditions for EM scattering problems," *Electronic Letters*, vol. 24, pp. 1093-1094, Aug. 18, 1988.
- [17] R. G. Rojas and Z. Al-Hekail, "Generalized impedance/resistive boundary conditions for electromagnetic scattering problems," *Radio Science*, vol. 24, pp. 1-12, Jan. /Feb. 1989.
- [18] J. -M. L. Bernard, "Diffraction by a metallic wedge covered with a dielectric material," *Wave Motion*, vol. 9, pp. 543-561, Nov. 1987.
- [19] R. Tiberio, R. Bessi, G. Manara, and G. Pelosi, "Scattering by a strip with two face impedances at edge-on incidence," *Radio Science*, vol. 17, pp. 1199-1210, Sept. / Oct. 1982.
- [20] H. J. Bilow, "Scattering by an infinite wedge with tensor impedance boundary conditions – a moment method/physical optics solution for the currents," *IEEE Trans. Antennas Propagat.*, vol. 39, pp. 767-773, Jun. 1991.

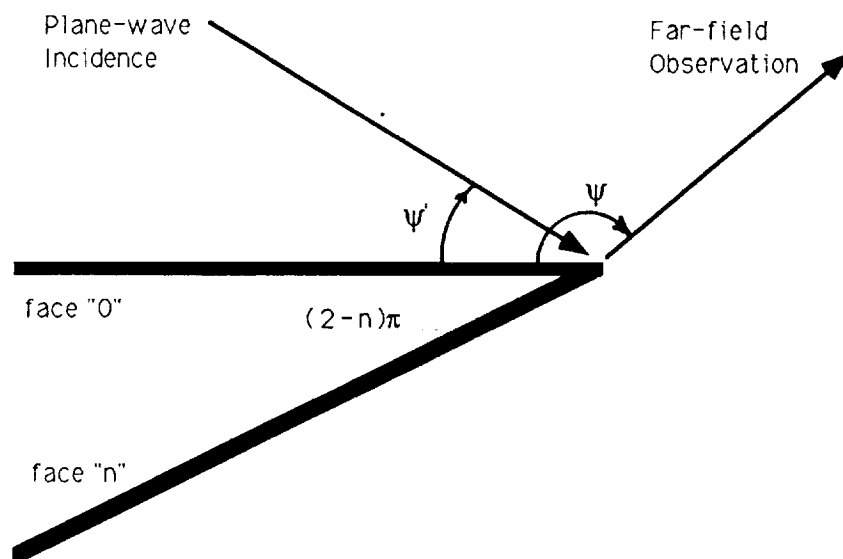


Fig. 1. Impedance wedge geometry.

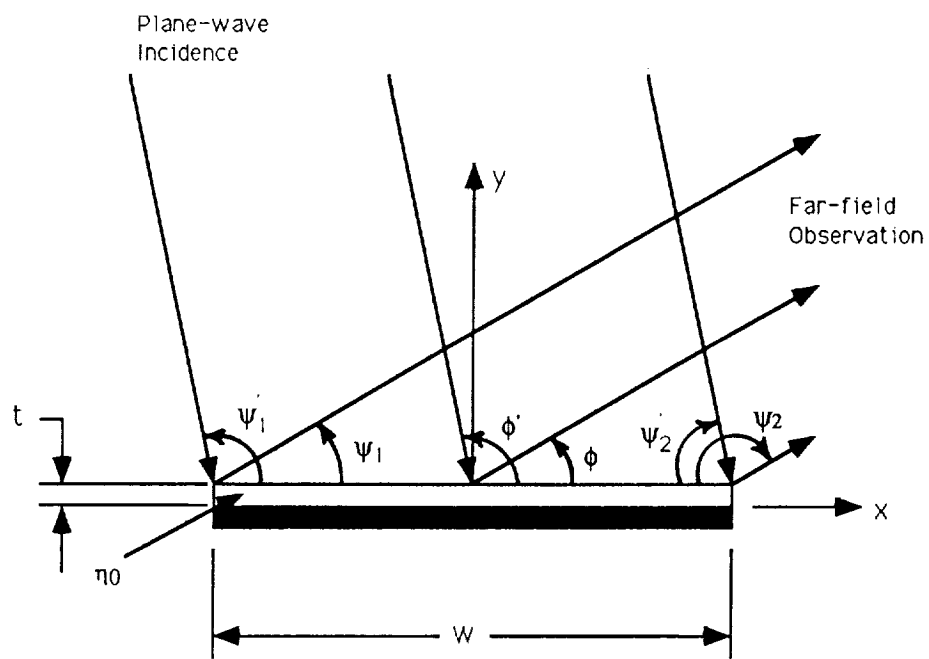


Fig. 2. Geometry for principal-plane scattering from a strip/plate with a finite-thickness coating backed by a perfect conductor.

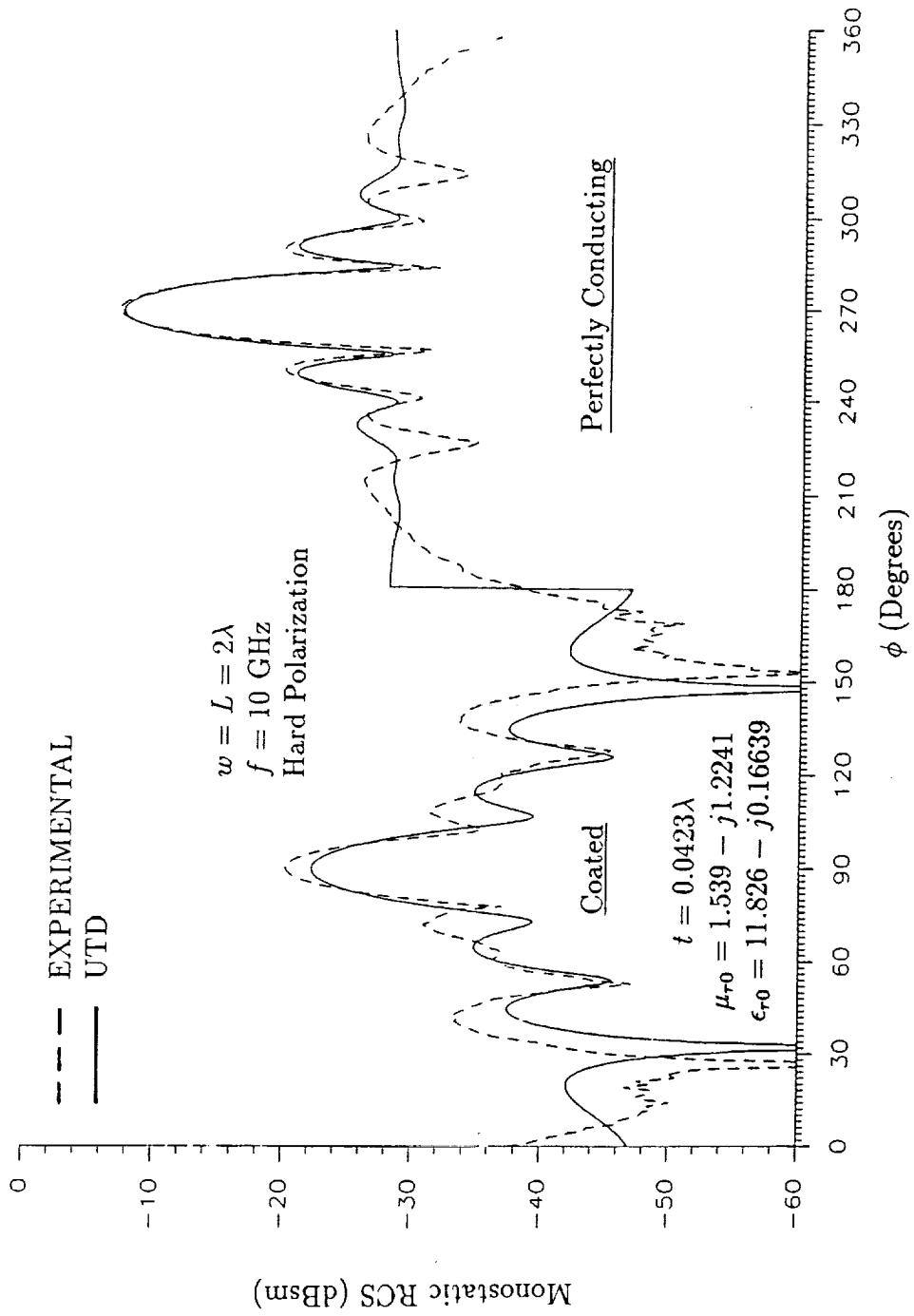


Fig. 3. Principal-plane, monostatic RCS of a coated plate.